



UNIVERSITÀ DI PARMA

ARCHIVIO DELLA RICERCA

University of Parma Research Repository

Metadynamics for perspective drug design: Computationally driven synthesis of new protein-protein interaction inhibitors targeting the EphA2 receptor

This is the peer reviewed version of the following article:

Original

Metadynamics for perspective drug design: Computationally driven synthesis of new protein-protein interaction inhibitors targeting the EphA2 receptor / Incerti, Matteo; Russo, Simonetta; Callegari, Donatella; Pala, Daniele; Giorgio, Carmine; Zanotti, Ilaria; Barocelli, Elisabetta; Vicini, Paola; Vacondio, Federica; Rivara, Silvia; Castelli, Riccardo; Tognolini, Massimiliano; Lodola, Alessio. - In: JOURNAL OF MEDICINAL CHEMISTRY. - ISSN 0022-2623. - 60:2(2017), pp. 787-796. [10.1021/acs.jmedchem.6b01642]

Availability:

This version is available at: 11381/2821075 since: 2021-10-11T17:28:34Z

Publisher:

American Chemical Society

Published

DOI:10.1021/acs.jmedchem.6b01642

Terms of use:

openAccess

Anyone can freely access the full text of works made available as "Open Access". Works made available

Publisher copyright

(Article begins on next page)

Metadynamics for Perspective Drug Design: Computationally Driven Synthesis of New Protein- Protein Interaction Inhibitors Targeting the EphA2 Receptor

*Matteo Incerti,^{‡1} Simonetta Russo,^{‡1} Donatella Callegari,¹ Daniele Pala,^{1†} Carmine Giorgio,¹
Ilaria Zanotti,¹ Elisabetta Barocelli,¹ Paola Vicini,¹ Federica Vacondio,¹ Silvia Rivara,¹
Riccardo Castelli,¹ Massimiliano Tognolini,^{*1} and Alessio Lodola^{*1,2}*

¹Dipartimento di Farmacia, Università degli Studi di Parma, Parco Area delle Scienze 27/A,
43124 Parma, Italy

²Department of Applied Sciences, Faculty of Health and Life Sciences, Northumbria University,
Newcastle upon Tyne, NE1 8ST, United Kingdom

ABSTRACT

Metadynamics (META-D) is emerging as a powerful method for the computation of the multidimensional free-energy surface (FES) describing the protein-ligand binding process. Herein, the FES of unbinding of the antagonist *N*-(3 α -hydroxy-5 β -cholan-24-oyl)-L- β -homotryptophan (UniPR129) from its EphA2 receptor was reconstructed by META-D simulations. The characterization of the free-energy minima identified on this FES proposes a binding mode fully consistent with previously reported and new structure-activity relationship data. To validate this binding mode new *N*-(3 α -hydroxy-5 β -cholan-24-oyl)-L- β -homotryptophan derivatives were designed, synthesized and tested for their ability to displace ephrin-A1 from the EphA2 receptor. Among them two antagonists, namely compounds **21** and **22**, displayed high affinity versus the EphA2 receptor and resulted endowed with better physicochemical and pharmacokinetic properties than the parent compound. These findings highlight the importance of free-energy calculations in drug design confirming that META-D simulations can be used to successfully design novel bioactive compounds.

INTRODUCTION

The EphA2 receptor is a member of the Eph receptor superfamily of receptor tyrosine kinases¹ and its biological activity is primarily controlled by a membrane-bound protein known as ephrin-A1.² The EphA2 receptor is highly expressed in a large number of cancer types, including melanoma, prostate, breast, colon, lung, pancreatic, and lung cancers.³ Recent evidence indicates that both EphA2 and its ephrin-A1 ligand are implicated in carcinogenesis⁴ as they promote the self-renewal of tumor-propagating cells, the acquisition of a migratory phenotype, and the formation of new blood vessels.⁵ Furthermore, the abnormal activation of EphA2 in tumor cells has been linked to vasculogenic mimicry,^{6,7} a process in which vascular channels are not formed by endothelial cells but rather by metastatic and genetically deregulated tumor cells. In this scenario, the EphA2 receptor has emerged as a promising target for the development of new and yet alternative antiangiogenic therapies.⁸ In principle, two key strategies can be used to inhibit the tumorigenic activity of the EphA2 receptor. The first one is based on the use of classical ATP-mimicking agents directed at the intracellular kinase domain of Eph receptor.⁹ The second one is based on molecular agents targeting the extracellular ligand-binding domain of EphA2, thus preventing its direct interaction with ephrin-A1.^{10,11} Some small molecules acting with this mechanism of action have been reported in the literature.^{12,13,14} Among them, lithocholic acid¹⁵ (LCA, Chart 1) and its analogues were identified as competitive and reversible antagonists of the EphA2 receptor, active in prostate cancer cells (PC3) at non-cytotoxic concentration.¹⁶ Starting from LCA, we recently synthesized a set of amino acid conjugates able to interfere with the EphA2–ephrin-A1 interaction with potency in the low micromolar range.¹⁷ In this series, *N*-(3 α -hydroxy-5 β -cholan-24-oyl)-L- β -homotryptophan (UniPR129, compound **16**, Chart 1) emerged as a particularly active EphA2 antagonist able to suppress angiogenesis in human umbilical vein

endothelial cells (HUVECs) through selective interaction with EphA2 receptor.¹⁸ Despite its promising pharmacodynamic profile,¹⁹ Compound **16** possesses some unfavorable physicochemical properties (i.e., high lipophilicity and low solubility), which have limited the study of this compound *in vivo*.²⁰

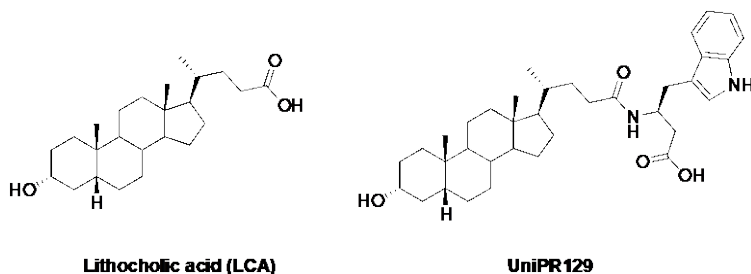


Chart 1. Structures of reference EphA2 receptor antagonists.

To improve the physicochemical properties of this class of steroidal-based ligands while maintaining or increasing their affinity for the EphA2 receptor, the knowledge of the atomistic mechanism of action of compound **16** becomes fundamental. On the other hand, the poor physicochemical profile of **16** has so far hampered the atomic resolution of the EphA2-compound **16** complex by X-ray and NMR spectroscopy. Therefore, the combination of free-energy simulations,^{21,22} either based on metadynamics (META-D)²³ or other enhanced sampling methods,^{24,25} and extensive structure-activity relationship (SAR) analysis^{26,27,28} appears as an alternative, viable approach to propose a reasonable model of interaction, exploitable in prospective drug design.^{29,30} META-D is currently emerging as a powerful enhanced sampling method³¹ for the efficient and rapid computation of multidimensional free-energy surfaces (FES) describing the protein-ligand binding process.^{32,33} This FES provides information on the position and energetics of minima such as the bound and the unbound states of a protein-ligand system allowing to retrieve the equilibrium binding free energy (ΔA_{bind}) which is related to the affinity of a ligand for its target. Moreover, this FES allows to identify minimum binding geometries of

the protein-ligand complex that can be used to design novel compounds for the target under investigation. In the present work, we expanded the current knowledge of SAR around both the amino acid portion and the 5 β -cholan-24-oic nucleus of **16**, reporting the synthesis and the biological activity of new LCA amino acid conjugates. The biological data were used to develop a reliable atomistic model of interaction between the lead compound **16** and the EphA2 receptor. The proposed molecular model was computationally validated by means of META-D simulations and exploited to design novel EphA2 receptor antagonists. Anticipating our results, a small set of new EphA2 antagonists, equally or slightly more potent than **16** with improved physicochemical properties or metabolic stability were identified. The present work underlines the potential of enhanced sampling methods in lead optimization campaigns.^{34,35}

Results and Discussion

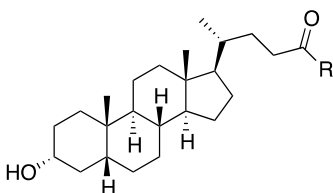
SAR analysis of amino acid conjugates of LCA

We started our SAR exploration on LCA amino acid conjugates by investigating the importance of the spacer connecting the terminal carboxylic acid to the amide group. The IC₅₀ values (μ M) of tested compounds together with their 95% confidence interval and with the polar surface area (PSA)³⁶ values are reported in Table 1. Conjugation of lithocholic acid (LCA) with glycine provided a compound (**2**) able to displace ephrin-A1 from the immobilized EphA2 receptor with a potency (IC₅₀ = 49 μ M) comparable to that of LCA (**1**). Compound **3**, obtained by conjugation of LCA with β -alanine, showed a moderate improvement in the inhibitory potency (IC₅₀ = 29 μ M), consistently with binding data reported in references 17 and 21. However, a further lengthening of the spacer resulted detrimental for binding the EphA2 receptor, as indicated by the barely detectable activity of compounds **4** and **5** (IC₅₀ > 100 μ M).

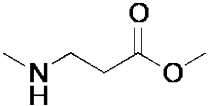
Analyzing the role of the terminal carboxylic group, we found that replacement of the carboxylic acid of compound **3** with a sulfonic acid (**6**) or its functionalization into a methyl ester (compound **7**) led to a loss in the inhibitory potency, suggesting that the presence of a free carboxylic group is critical for the inhibition of EphA2-ephrin-A1 association. Given these preliminary results, we focused our work on the synthesis of β -alanine conjugates of LCA (Table 2) bearing lipophilic chains of different size, shape and electronic properties. Aliphatic side chains, either linear (compound **8**) or branched (compounds **9** and **10**) ones, were inserted at the β position of the amino acid moiety of compound **3**. Among them, only the β -homovaline derivative **9** resulted slightly more potent than compound **3**. Similarly, the introduction of a phenyl (**11**), a benzyl (**12**), or a phenylethyl (**13**) substituent gave unsatisfactory results considering that **11** and **12** resulted moderately more potent than **3**. A significant improvement in the inhibitory potency was instead obtained introducing larger aryl side chains. Single digit micromolar IC_{50} values were observed for the α -naphthylmethyl derivative **14** and the benzo[*b*]thiophen-3-ylmethyl one **15**. This improvement in the inhibitory potency could be ascribed to the ability of the naphthyl and benzothiophene nuclei to undertake productive steric and/or electrostatic interactions with an accessory pocket of the EphA2 binding site. A further enhancement in the potency was obtained with the indol-3-ylmethyl derivative **16**. The inhibitory potency of this compound approached the sub-micromolar range ($IC_{50} = 0.91 \mu\text{M}$). Although the NH group of the indole group has been proposed to be a weak H-bond donor,³⁷ we attributed the slightly higher activity of **16**, compared to that of **14** and **15**, to the ability of this NH to form an additional H-bond within the EphA2 receptor. To support this hypothesis, the diastereoisomer of **16**, in which the chirality of the β carbon bearing the indol-3-ylmethyl chain was inverted, was synthesized and tested. Compound **17**, which likely projects the indol-3-ylmethyl chain in

another region of EphA2 binding site, thus failing to undertake a H-bond with the receptor, resulted 25-fold less potent than **16**, supporting our working hypothesis.

Table 1. IC₅₀ values for LCA and its linear amino acid conjugates 2-7 obtained from EphA2-ephrin-A1 displacement experiments.^a

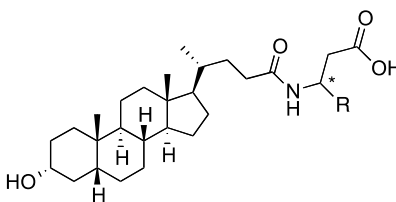


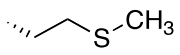
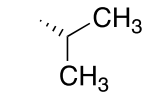
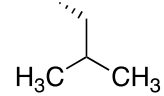
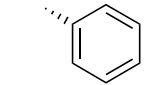
Cpd.	R-	IC ₅₀ (μM) ^{b,c}	PSA (Å ²) ^d
1 (LCA)		79 [67-93]	72
2		49 [42-58]	109
3		29 [23-36]	111
4		inactive ^b	106
5		inactive ^b	106
6		72 [53-100]	119

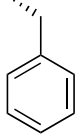
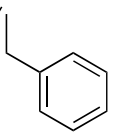
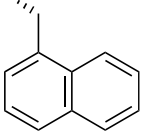
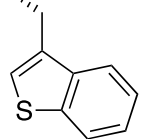
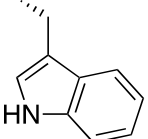
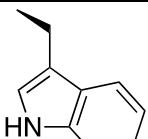
7		inactive ^c	91
---	---	-----------------------	----

^a Compounds **2** and **3** have been described in references 17 and 21, respectively. ^b Values are the mean from at least three independent experiments. ^b Numbers in brackets denote the 95% confidence interval for IC₅₀. ^c No signal detected up to 100 μM. ^d Polar surface area calculated with QikOrop³⁸ obtained from minimized 3D-structures of the listed compounds.

Table 2. IC₅₀ values of β-substituted β-alanine conjugates of LCA obtained from EphA2-ephrin-A1 displacement experiments.



Cpd.	R-	IC ₅₀ (μM) ^{a,b}	PSA (Å ²) ^c
3	H	29 [23-36]	111
8		83 [50-138]	104
9		10 [6.6-16]	96
10		inactive ^b	105
11		14 [10-20]	104

12		18 [12-26]	104
13		inactive ^b	98
14		3.9 [3.0-5.0]	104
15		1.8 [1.5-2.1]	102
16		0.91 [0.80-1.1]	120
17		26 [18-37]	123

^a Values are the mean from at least three independent experiments. ^bNumbers in brackets denote the 95% confidence interval for IC₅₀. ^c No signal detected up to 100 μM. ^c Polar surface area calculated with QikProp obtained from minimized 3D-structures of the listed compounds.

Free-energy simulations

The availability of the X-ray structure of the EphA2 receptor³⁹ prompted us to investigate the binding mode of compound **16** by atomistic simulations. Flexible docking of **16** within the EphA2 receptor failed to produce a binding pose able to satisfactorily explain the SARs for β-alanine conjugates (Table 2). In particular, it was not possible to identify a specific interaction

for the indole ring of **16** that could account for its higher inhibitory potency compared to those of analogues **14**, **15** and **17**. As the inclusion of both conformational flexibility and solvent reorganization are often fundamental to get a reasonable guess of a protein-ligand binding arrangement,^{40,41} we performed molecular dynamics (MD) simulations (see Methods for details) starting from the top-ranked solution of **16** obtained with Glide⁴² software (Figure 2A and Figure S1). A 30 ns-long simulation revealed that the docked conformation was not stable within the EphA2 active site as indicated by its high root-mean-square deviation (RMSD) observed after only 5 ns of simulation (Figure 2B). On the other hand, the same MD identified an alternative arrangement of **16** (*vide infra*) whose geometry was maintained for nearly 25 ns of simulation. In this new arrangement (Figure 3A and Figure S2), the indole ring of **16** was inserted in a solvent-exposed pocket of EphA2 delimited by Phe108, Cys70, Val69 and Asp53. The proximity of the β -alanine substituent to the hydrophobic side of the pocket formed by Phe108, Cys70 and Val69 could explain the improved potency of compounds bearing larger aromatic groups (i.e., compounds **14-16** vs compounds **8-13**) and the H-bond undertaken by the indole NH of **16** with the carboxylate group of Asp53 may be the reason for its higher potency compared with the benzo[*b*]thiophen-3-yl group of **14** or the α -naphthyl one of **15**. Moreover, the newly identified binding mode underlines the importance of having an N-acyl- β -alanine portion with a free carboxylate group capable of forming a tight network of interactions with the conserved Arg103 of EphA2. It is worth mentioning that docking simulations with Glide (either in SP or XP mode) were not able to produce a binding pose for **16** comparable to that observed during the MD simulation reported in Figure 3A.

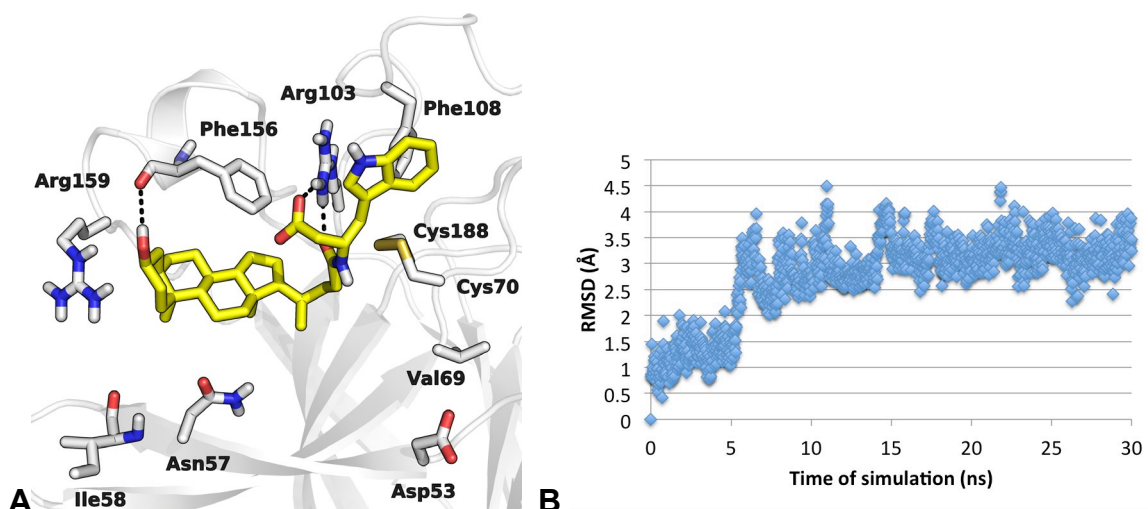


Figure 2. A) Compound **16** (yellow carbon atoms) within the high-affinity pocket of the EphA2 receptor (white cartoons, white carbon atoms) as obtained by docking with Glide. B) Root mean square deviation (RMSD) of heavy atom positions of compound **16** calculated from an MD simulation trajectory using the docked conformation of the ligand as reference structure.

To check the stability of this novel binding mode, we performed five independent runs of short MD simulations (for a total of 100 ns of simulations) using the EphA2-compound **16** complex depicted in Figure 3A as starting structure. The root mean-square deviation (RMSD) of the ligand remained below 2.5 Å in all the runs suggesting that this specific arrangement of the protein-ligand complex was in a well-defined free-energy minimum (Figure S3, Supporting information). To corroborate this model of interaction, we reconstructed the FES of unbinding for the EphA2-compound **16** complex by means of well-tempered META-D,⁴³ starting from the complex obtained by docking with Glide. META-D allows the compound to explore the whole binding site moving from one free-energy minimum to the others and then going back into the previous ones, overcoming the high free-energy barriers encountered during the binding process. From the final FES, all the accessible binding modes are identified and classified along a fairly

accurate free-energy scale.⁴⁴ To this end, we simulated the unbinding process following a computational protocol already successfully applied to study the interaction of EphA2 and LCA (reference 21), applying general collective variables,⁴⁵ i.e., the distance between the center of mass (CM) of EphA2 and the CM of compound **16** and the angle vector taken between the protein CM and the major inertia axis of the steroid moiety of **16**. Figure 3B reports the resulting FES of unbinding of **16** from the ligand-binding domain of EphA2 receptor. The surface identifies a profound free-energy minimum region corresponding to protein-ligand geometries (distance = 9.5 Å; angle= 100 °) resembling the binding mode proposed by the plain MD simulation and displayed in Figure 3A. On the same FES, geometries corresponding to the binding pose obtained by docking (Figure 2A) were observed in a high free-energy region (distance = 10 Å; angle= 130 °), in agreement with the poor structural stability of this arrangement observed during the plain-MD simulation. According to the shape of the FES, no other free-energy binding minima were detected. Conversely, a well-defined minimum corresponding to the (fully solvated) unbound state of the ligand was identified (distance > 20 Å; 60 < angle < 130 °), allowing us to estimate the Helmholtz free-energy of binding (ΔA_{bind}). The calculated ΔA_{bind} for the EphA2-compound **16** complex (-8.35 kcal/mol) was in reasonable agreement with the experimental one of -8.80 kcal/mol, deduced from the previously reported K_i ,¹⁸ supporting the validity of the proposed model of interaction.

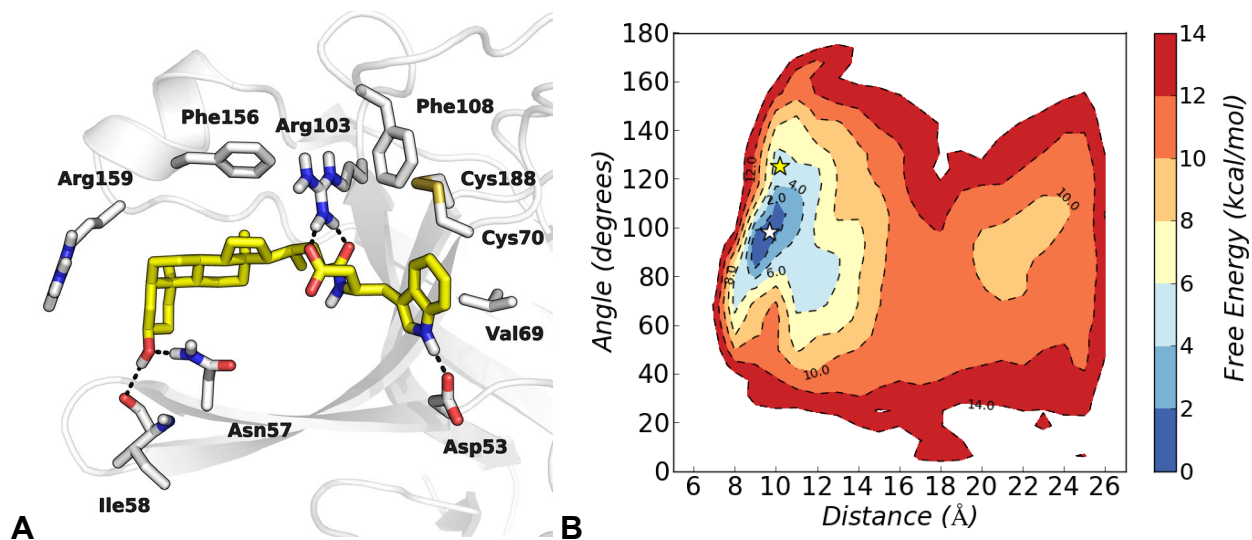


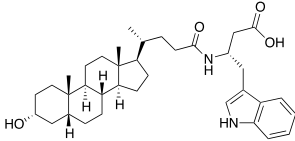
Figure 3. A) Most stable binding conformation of the EphA2-compound **16** complex observed in a 30 ns-long MD simulation starting from the docking complex depicted in Figure 2A. Compound **16** is depicted with yellow carbon atoms while EphA2 carbon atoms are in white. B) FES of unbinding of compound **16** from EphA2 reconstructed using metadynamics as a function of the distance between the CM of EphA2 and the CM of compound **16** and the angle vector taken between the protein CM and the major inertia axis of the steroid moiety of **16**. The yellow star indicates the binding mode identified by docking, while the white star indicates the position of the most stable binding mode identified by plain MD simulation.

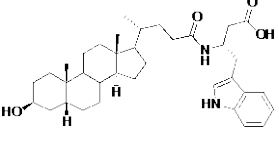
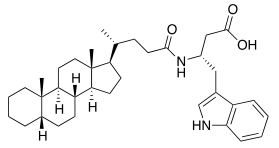
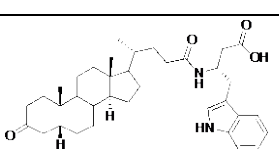
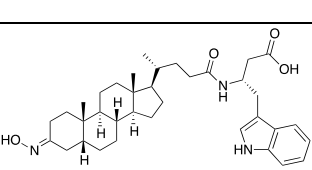
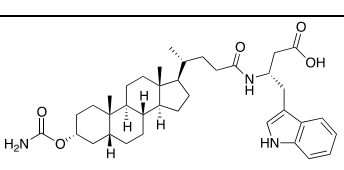
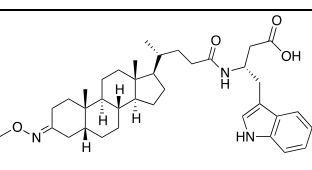
Binding mode validation: Design and testing of novel EphA2 antagonists

The binding mode depicted in Figure 3A highlights the importance of the 3 α -hydroxyl group of compound **16** for receptor binding. This group is indeed engaged in a H-bond network involving Asn57 side chain and Ile58 backbone. To confirm that the presence of a substituent with H-bond capability and with a specific spatial orientation is essential to maintain high inhibitory potency, we synthesized derivatives of compound **16** where the 3 α -hydroxyl group was replaced by a 3 β -hydroxyl one (**18**), was removed (**19**), or oxidized to a 3-keto group (**20**). In all these cases, a

significant drop in the inhibitory potency was observed (Table 3). Starting from the model of Figure 3A, we designed substituents in principle able to form a H-bond network comparable to that of the 3 α -hydroxyl group. Supported by the results of META-D simulations, we thus replaced the 3 α -hydroxyl group of **16** with a 3-hydroxyimino (**21**) or a 3 α -carbamoyloxy group (**22**). Indeed, simulations indicated that both the hydroxyimino and the carbamoyloxy groups were able to interact with Asn57 and Ile58 (Figure S4) and that their estimated free-energy of binding ΔA_{bind} for the EphA2 receptor of **21** and **22** was comparable with that of the reference compound **16** (*vide infra*). When tested in wet assay, these new compounds showed an inhibitory potency comparable or slightly higher than the lead compound **16**, with IC₅₀ values of 3.1 μM and 0.8 μM for **21** and **22**, respectively (Table 3). Again, removal of the H-bond donor group as in compound **23**, led to a reduction in the inhibitory potency confirming that position 3 of the steroidal nucleus is accommodated in a hydrophilic pocket of EphA2 with strict stereo-electronic requirements.

Table 3. IC₅₀ of 3-substituted 5 β -cholan-24-oyl-L- β -homotryptophan derivatives from EphA2-ephrin-A1 displacement experiments.

Cpd.	Structure	IC ₅₀ (μM) ^{a,b}	PSA (\AA^2) ^c
16		0.91 [0.80-1.1]	120

18		17 [13-24]	118
19		28 [22-35]	96
20		28 [22-36]	127
21		3.1 [2.8-3.6]	141
22		0.80 [0.51-0.98]	158
23		13 [8-20]	127

^a Values are mean from at least three independent experiments. ^bNumbers in brackets denote the 95% confidence interval for IC₅₀. ^c Polar surface area calculated with QikProp obtained from minimized 3D-structures of the listed compounds.

As a conclusive step of validation of our proposed model of interaction, we calculated the free-energy of binding of a small set of selected EphA2 inhibitors by means of well-tempered META-D and we analyzed their agreement with the experimental data. Binding free-energy obtained through well-tempered META-D has been reported to be within the range of chemical accuracy,⁴⁶ and thus useful for retrospective and perspective drug design studies.

Table 4 reports the calculated ΔA_{calc} for compound **3**, **15**, **16**, **17**, **19** and **22** along with their experimental pIC_{50} values. The computed ΔA_{calc} values well parallel inhibitory data on ephrin-A1 binding to EphA2 as indicated by the Pearson correlation coefficient (r) of 0.96. It is worth mentioning that while statistically significant (p -value < 0.05) such a correlation is based on a limited number of compounds ($n = 6$).

Table 4. pIC_{50} values, experimental binding free-energies (ΔG_{exp}) and calculated binding free-energies (ΔA_{calc}) for selected EphA2 antagonists.

Cpd.	$\text{pIC}_{50}^{\text{a}}$	ΔG_{exp} (kcal/mol) ^b	ΔA_{calc} (kcal/mol) ^c
3	4.54	-6.87	- 4.46
15	5.74	-8.57	- 7.65
16	6.04	-9.00	- 8.35
17	4.58	-6.93	-5.29
19	4.55	-6.88	- 3.35
22	6.10	-9.08	- 8.78

^a pIC_{50} values obtained from data reported in Tables 1 and 3. ΔG_{exp} values were obtained from $\Delta G_{\text{exp}} = -RT \ln K_i$, while K_i were deduced from IC_{50} value by applying the Cheng-Prusoff equation. ^c The convergence of META-D simulations was verified comparing the FES at different times of simulation (see Methods). In these conditions, the error associated to the estimation of ΔA_{calc} was lower than 0.5 kcal/mol.

Said that, the applied computational methodology was able to reproduce the gain in inhibitory potency obtained introducing the benzo[*b*]thiophen-3-ylmethyl chain in compound **15** (cfr. **3** and **15**) and replacing the sulfur atom in **15** with the NH group of **16**. Furthermore, these META-D simulations well reproduced the difference in the binding free energy between the reference antagonist **16** and its diastereoisomer **17** ($\Delta A_{\text{calc}} = -3.06$ kcal/mol vs $\Delta G_{\text{exp}} = -2.07$ kcal/mol). The binding geometry corresponding to the main free-energy minima found for the EphA2-compound **17** (Figure 4) indicates that the D- β - homotryptophan moiety of this compound failed

to undertake productive polar interactions with Asp53, which is instead targeted by the L- β -homotryptophan portion of **16**.

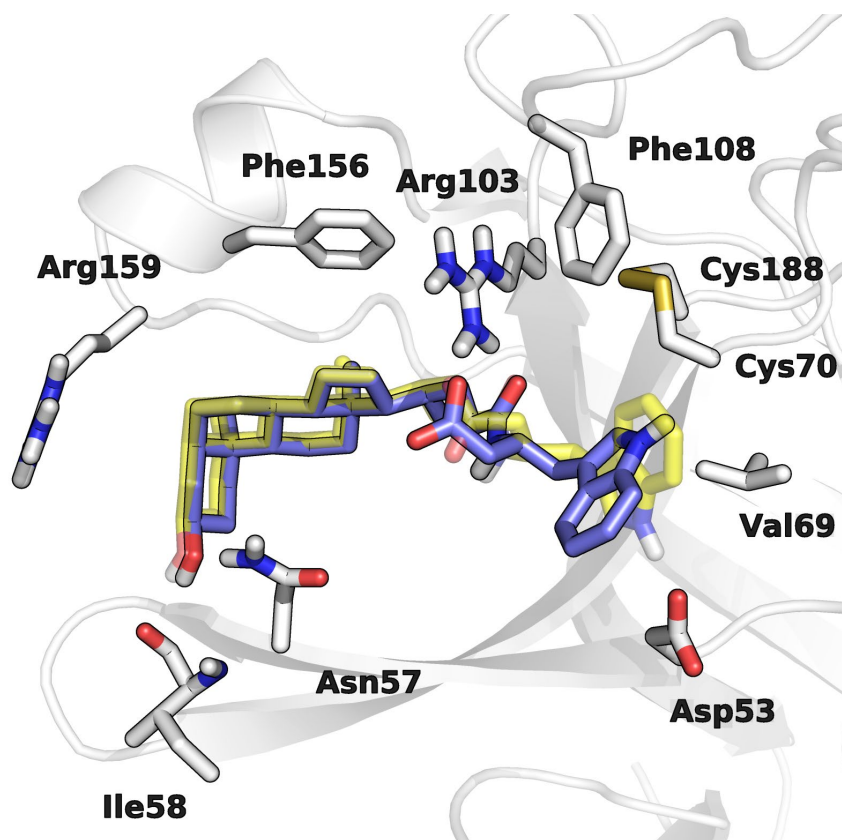


Figure 4. Representative binding free-energy minimum of the EphA2-compound **17** complex identified by META-D simulation. Compound **17** is represented with violet carbon atoms, while EphA2 atoms are reported in white. For comparison, the bound conformation of its diastereoisomer **16** (shaded yellow carbon atoms) is also reported.

Finally, the effect on the potency obtained through modification of position 3 of compound **16** was also well captured by our simulations, as indicated by the ΔA_{bind} values calculated for compounds **19** and **22**, with the former higher and the latter substantially equal to that of compound **16**.

Physicochemical properties and pharmacokinetics of selected EphA2 antagonists

Computer-aided exploration of the SAR around the *N*-(3 α -hydroxy-5 β -cholan-24-oyl)-L- β -homotryptophan nucleus of compound **16**, allowed to identify two effective EphA2 antagonists (i.e., compounds **21** and **22**) possibly endowed with improved in vitro ADME properties according to their slightly higher polar surface area (PSA, Table 3).⁴⁷ We therefore evaluated the plasma concentrations of compounds **21** and **22** following oral administration to mice. In fact, the parent compound **16**, while endowed with a lipophilicity (i.e., the distribution coefficient in *n*-octanol/buffer at pH 7.4, Table 5) compatible with oral absorption,⁴⁸ barely reached detectable plasma levels (i.e. < 0.01 μ M) after oral administration to mice at 30 mg/kg (Figure 5).

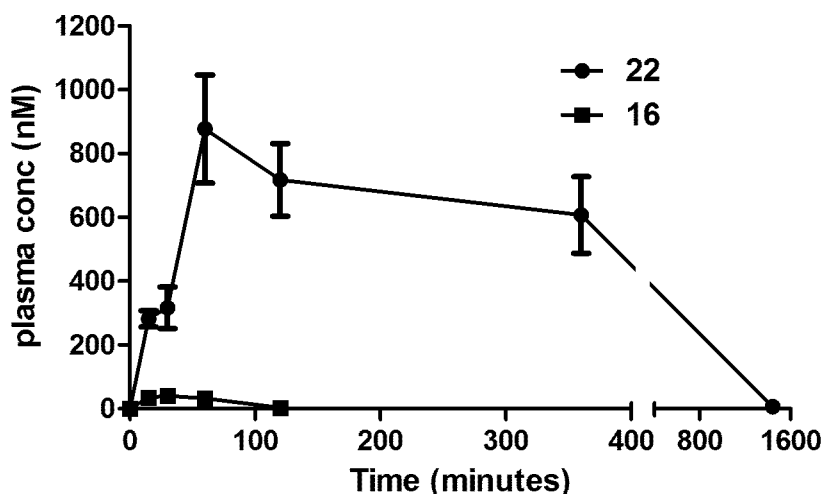


Figure 5. Plasma profiles of compounds **22** (black circles) and **16** (black squares). Compound concentrations (μ M) are reported over 1440 minute (24 h) for **22** and 120 min for **16**. Data are the means of at least four independent experiments \pm SEM.

A further analysis of its properties revealed that while **16** possesses both a fair kinetic solubility ($31.8 \pm 4.2 \mu$ M) and high mouse plasma stability (% of recovered compound close to 100 after

24 h of incubation), it suffers from rapid degradation in mouse liver microsomes ($t_{1/2} = 16.8 \pm 1.5$ min), mainly due to the oxidation of the carbon at position 3. HPLC–ESI-MS/MS data indeed confirmed that the main metabolite of **16** is its 3-keto analogue **20** (data not shown). Compounds **21** and **22**, being not susceptible to oxidation at position 3 displayed a greater metabolic stability in mouse liver microsomes ($t_{1/2}$ of 60.4 ± 9.3 min for **21** and 156.3 ± 10.1 min for **22**) and reached higher levels in vivo, with C_{\max} of 0.40 ± 0.10 (reached at 1 h, data not shown) and 0.87 ± 0.25 μM (reached at 1 h, Figure 5), respectively, after oral administration to mice at 30 mg/kg. These results thus indicate that the introduction of polar groups different from the 3α -hydroxyl one is an effective strategy to maintain good inhibitory potency on EphA2 while gaining a higher oral bioavailability in mice.

Table 5. Physicochemical properties, in vitro metabolic stability and in vivo concentration of selected compounds.

Cpd.	$\log D_{\text{Oct},7.4}$	Solubility ^a (μM)	Plasma stability % after 24 h	Liver stability ^b $t_{1/2}$ (min)	In vivo C_{\max} (μM) ^c
16	4.90 ± 0.15	31.8 ± 4.2	98.3 ± 9.5	16.8 ± 1.5	0.01 ± 0.01
21	4.23 ± 0.11	51.9 ± 4.4	93.7 ± 11.3	60.4 ± 9.3	0.40 ± 0.10
22	5.01 ± 0.20	18.7 ± 3.4	98.2 ± 2.5	156.3 ± 10.1	0.87 ± 0.25

^a From DMSO stock solution. Final DMSO concentration in 50 mM MOPS buffer pH 7.4: 1%. ^b Mouse liver microsomes. ^c Compounds (30 mg/kg) were orally administered to at least 4 fasted mice.

CONCLUSIONS

META-D methods show great promise in elucidating the mode of action and in computing the change in free energy associated with the binding of small molecules to their target. However, META-D techniques have been so far applied in retrospective studies of protein ligand binding. The ability of different META-D protocols to reproduce available experimental data suggest that the time has now come to use metadynamics in prospective drug design efforts, with a particular focus on lead optimization.³⁰ With this in mind, we show here that information gained from SAR exploration of 5 β -cholan-24-oyl-L- β -homotryptophan derivatives combined with the characterization of the FES of unbinding of the reference compound **16** obtained by META-D allowed to discover two novel antagonists (compounds **21** and **22**) targeting the EphA2 receptor with inhibitory potency in the low micromolar range and, more importantly, with higher polarity, likely responsible for their good metabolic stability and oral bioavailability in mice. These results highlight the power of META-D simulations in the rational design of novel active compounds with improved pharmacological properties.

EXPERIMENTAL SECTION

Model building

Docking simulations were performed starting from the crystal structure of the EphA2–ephrin-A1 complex (3HEI.pdb).³⁹ The EphA2–ephrin-A1 complex was submitted to a protein preparation procedure using Maestro 10.5 software.⁴⁹ This approach includes addition of missing side chains and hydrogen atoms, assignment of the tautomeric state of histidine residues to maximize the number of hydrogen bonds, assignment of the protonation state of titratable amino acids at physiological pH, and geometric optimization of the whole system to a RMSD value of 0.3 Å. At the end of this procedure, ephrin-A1 ligand and solvent molecules were deleted from the EphA2 binding site and the resulting protein structure was employed to build a docking grid

with Glide 7.0.⁵⁰ The grid was centred on the ligand-binding domain of EphA2, in a region delimited by Arg103, Phe156 and Arg159, using enclosing and bounding boxes of 20 and 14 Å on each side, respectively. The atomistic model of compound **16** was built with Maestro and its geometry was optimized by energy minimization using OPLS2005 force field⁵¹ to a gradient of 0.01 kcal mol⁻¹ Å⁻². Docking simulations were then performed using Glide 7.0, starting from minimized structures of compound **16**. The best-ranked solution (according to the standard precision G_{score}) was selected and the resulting complex with EphA2 was submitted to MD simulation. To this end, the EphA2-compound **16** complex was solvated by 7096 TIP3P water molecules and its total charge neutralized by adding 6 Na⁺ ions. The final system was composed by 24144 atoms. All bond lengths to hydrogen atoms were constrained using M-SHAKE. Short-range electrostatic interactions were cut off at 9 Å, whereas long-range electrostatic interactions were computed using the Particle Mesh Ewald method.⁵² A RESPA integrator was used with a time-step of 2 fs, and long-range electrostatics were computed every 6 fs. The solvated complex was equilibrated using 5-ns long molecular dynamics simulations in the NPT ensemble at 1 atm and 300 K followed by 5 ns of simulations in the NVT ensemble at 300 K using the Langevin thermostat.⁵³ A production run of 30 ns in NVT condition was then performed at 300 K again with the Langevin thermostat. All the MD simulations were performed using Desmond 4.5 software⁵⁴ in combination with the OPLS2005 force field.

Molecular models of EphA2 in complex with compounds **3**, **15**, **17**, **19** and **22** were built starting from the conformation of EphA2 obtained at the end of the plain MD simulation of the EphA2-compound **16** complex (Figure 3A). A new docking grid was build, using the same protocol previously described and the minimized structures of compounds **3**, **15**, **17**, **19** and **22** were docked into the new grid using Glide 7.0. The best docked poses were selected and the

resulting EphA2-inhibitor systems were *i.* solvated with TIP3P water molecules, *ii.* neutralized by adding 6 Na⁺ ions, and *iii.* equilibrated by 5-ns long molecular dynamics simulations in the NPT ensemble at 1 atm and 300 K followed by 5 ns of simulations in the NVT ensemble at 300 K using the Langevin thermostat.

Well-tempered META-D simulations of protein-ligand unbinding

Well-tempered META-D simulations in the NVT ensemble were performed starting from the five equilibrated EphA2-inhibitor complexes. The simulations were performed with Desmond 4.5 software in combination with the OPLS2005 force field. The META-D biasing potentials were added on two distinct collective variables (CVs) relevant for ligand unbinding, namely the distance between the center of mass (CM) of the EphA2 ligand-binding domain and the CM of the ligand steroid moiety, and the angle vector taken between the same protein reference point and the major inertia axis of the steroid moiety. Gaussians were deposited every 0.25 ps, with a starting height of 0.15 kcal/mol and gradually decreased on the basis of adaptive bias with a ΔT of 1200 K. The width of the Gaussians was 0.5 Å for the distance and 2.5 degrees for the angle. We considered the well-tempered META-D simulations ended when the height of the deposited Gaussian in the space of the employed CVs decreased close to zero.⁴³ For practical reasons, a cut-off of 0.01 kcal/mol, corresponding to a residual height of the Gaussian smaller than the 10% of the initial height, was applied to define the end of the well-tempered META-D simulation, similarly to what performed in reference 55. We verified that the META-D simulations were converged by comparing the FES at different times of simulation once the cut-off in the Gaussian height was reached. In these conditions, the error associated to the estimation of ΔA_{bind} was lower than 0.5 kcal/mol. All the well-tempered META-D simulations converged in less than 100 ns.

Chemistry

Unless otherwise noted, reagents and solvents were purchased from commercial suppliers (Aldrich and AlfaAesar) and were used without purification. The progress of the reaction was monitored by thin-layer chromatography with F₂₅₄ silica-gel precoated sheets (Merck Darmstadt, Germany). UV light and a solution of ammonium molybdate and ceric sulfate in aqueous sulfuric acid (5% v/v) were used for detection. Flash chromatography was performed using Merck silica-gel 60 (Si 60, 40-63 μm , 230-400 mesh ASTM). Dichloromethane was dried by distillation over calcium hydride. All reactions were carried out using flame-dried glassware under atmosphere of nitrogen. Melting points were determined on a Gallenkamp melting point apparatus and were not corrected. The ¹H-NMR and ¹³C-NMR spectra were recorded on a Bruker Avance 400 spectrometer (400MHz); chemical shifts (δ scale) are reported in parts per million (ppm). ¹H-NMR spectra are reported in the following order: multiplicity, approximate coupling constants (*J* value) in Hertz (Hz) and number of protons; signals were characterized as s (singlet), d (doublet), t (triplet), q (quartet), m (multiplet), bs (broad signal). Mass spectra were recorded on an Applied Biosystem API-150 EX system spectrometer with ESI interface. Compounds **2-23** were prepared according to the synthetic procedures described in the supporting information. The purity of each compound was assessed by HPLC/MS analysis and shown to be 95% or higher. Compounds bearing an azomethinic group in position 3 resulted a mixture of the two isomeric forms *E* and *Z*. The rapid interconversion between these two forms didn't allow the separation of the pure single isomers. The attribution of the ¹H-NMR the peaks were done considering the most abundant isomer, while in the ¹³C-NMR spectra all the detected peaks were reported.

Pharmacology

ELISA assays and IC₅₀ determination on EphA2-ephrin-A1 binding

ELISA assays were performed as previously described.¹⁵ Briefly, 96-well ELISA high binding plates (Costar #2592) were incubated overnight at 4 °C with 100 µL/well of 1 µg mL⁻¹ EphA2-Fc (R&D 639-A2) diluted in sterile phosphate buffered saline (PBS, 0.2 g L⁻¹ KCl, 8.0 g L⁻¹ NaCl, 0.2 g L⁻¹ KH₂PO₄, 1.15 g L⁻¹ Na₂HPO₄, pH 7.4). Next day the wells were washed with washing buffer (PBS + 0.05% tween20, pH 7.5) and blocked with blocking solution (PBS + 0.5% BSA) for 1 hour at 37 °C. Compounds were added to the wells at proper concentration in 1% DMSO and incubated at 37 °C for 1 h. Biotinylated ephrin-A1-Fc (R&D Systems BT602) was added at 37 °C for 4 h at its K_D value in displacement assays or in a range from 1 to 2000 ng mL⁻¹ in saturation studies. Then wells were washed and incubated with 100 µL/well Streptavidin-HRP (Sigma S5512) for 20 minutes at room temperature, washed again and finally incubated at room temperature with 0.1 mg mL⁻¹ tetramethylbenzidine (Sigma T2885) reconstituted in stable peroxide buffer (11.3 g L⁻¹ citric acid, 9.7 g L⁻¹ sodium phosphate, pH 5.0) and 0.02% H₂O₂ (30% m/m in water), added immediately before use. The reaction was stopped with 3N HCl 100 µL/well and the absorbance was measured using an ELISA plate reader (Sunrise, TECAN, Switzerland) at 450 nm. IC₅₀ values were determined using one-site competition non-linear regression analysis with Prism software (GraphPad Software Inc.).

Lipophilicity. Distribution coefficients (Log $D_{\text{oct},7.4}$) values in the *n*-octanol/buffer partition system were measured at room temperature (25±3°C) via the reference shake-flask method. Buffer was 50 mM MOPS (3-morpholinopropanesulfonic acid), pH 7.4, 0.15 M ionic strength for KCl addition. Tested compounds, after equilibrating overnight between pre-saturated partition phases, were analyzed by HPLC-ESI-MS/MS, after dilution of each partition phase with

MeOH, containing the Internal Standard (IS) *N*-(3 α -hydroxy-5 β -cholan-24-oyl)-L-tryptophan.¹⁷ Log $D_{\text{Oct},7.4}$ values reported in Table 5 are the means of three independent partition experiments, employing different n-octanol/buffer volume ratios.

Kinetic solubility measurements. 10 mM stock solutions of compounds **16**, **21**, **22** were freshly prepared in DMSO. Samples for solubility measurements were prepared in a 96-well plate format by adding 2 μL of DMSO stock solution to 198 μL of 50 mM MOPS, pH 7.4, 0.15M ionic strength for KCl addition. Final DMSO percentage was kept constant to 1%. Samples were left into agitation for 4 h at room temperature (25 ± 3 °C), centrifuged (1,000 g, 10 min, 20 °C), an aliquot of the supernatant was diluted 1:1 with MeOH containing the Internal Standard *N*-(3 α -hydroxy-5 β -cholan-24-oyl)-L-tryptophan and injected into HPLC-ESI-MS/MS system for quantification. Dissolved concentrations were quantified by means of calibration curves built for each compound in MeOH.

Plasma stability. Mouse plasma was quickly thawed and diluted to 80% (v/v) with 100 mM Phosphate Buffered Saline (PBS) pH 7.4 to control pH over the time period of the experiments. Stock solutions of compounds **16**, **21** and **22** in DMSO were added (compound concentration: 1 μM , DMSO concentration: 1% v/v) and maintained at 37 °C. At regular time points, aliquots of plasma solution were sampled, two volumes of MeCN were added, samples were centrifuged (9,000 g, 10 min, 4 °C) and analyzed by HPLC-ESI-MS/MS for percentage of remaining compound over incubation time.

Mouse liver microsomal stability. Stock solutions of compounds **16**, **21** and **22** were prepared in DMSO immediately before use; co-solvent concentration in final samples was kept at 1% v/v. Stability was evaluated by incubation of 1 μM of selected compounds in the presence of mouse liver microsomes (1 mg protein ml^{-1}), at 37 °C, in the presence of a NADPH-

regenerating system (2 mM NADP⁺, 10 mM glucose-6-phosphate, 0.4 U mL⁻¹ glucose-6-phosphate dehydrogenase, 5 mM MgCl₂) in 100 mM PBS buffer solution pH 7.4. The reaction mixtures were preheated (37 °C) for 5 min before adding the compound. At fixed time points (t = 0; 15; 30; 45; 60 min), aliquots of samples were withdrawn, deproteinized with two volumes of acetonitrile, centrifuged and the supernatant analyzed by injection in HPLC-ESI-MS/MS system.

In vivo dosages. Compounds **16** and **22** were formulated in 0.5% methylcellulose (10/90 v/v) for the oral administration. Test compounds were orally dosed as a single esophageal gavage at 30 mg/kg to male mice. Each group consisted of four mice. Blood samples were collected via tail puncture at 5-7 time points in the following range: 15 min–1440 min (oral route). Whole blood samples were centrifuged at 5000 rpm for 10 min, and the resulting plasma samples were stored at –20 °C pending analysis. Compounds were dosed by HPLC-ESI-MS/MS employing a Thermo Accela UHPLC gradient system coupled to a Thermo TSQ Quantum Access Max triple quadrupole mass spectrometer equipped with a heated electrospray ionization (H-ESI) ion source. Xcalibur 2.1 software was used for sample injection, peaks integration, and quantification.

AUTHOR INFORMATION

Corresponding Author

* Phone: +39 0521 905062. Fax: + 39 0521 905006. E-mail: alessio.lodola@unipr.it

* Phone: +39 0521 906021. Fax: + 39 0521 905006. E-mail: massimiliano.tognolini@unipr.it

Present Addresses

†Chiesi Farmaceutici S.p.A. Largo Belloli, 11 A, Parma, Italy.

Author Contributions

The manuscript was written through contributions of all authors. All authors have given approval to the final version of the manuscript. ‡These authors contributed equally.

Notes

MI, AL and MT filed a patent application related to the synthesis and use of Eph-ephrin receptor antagonists. Authors will release the atomic coordinates and experimental data upon article publication.

ACKNOWLEDGMENT

This work was supported by Ministero dell'Università e della Ricerca, “Futuro in Ricerca” program (project code: RBFR10FXCP) to AL and Associazione Italiana Ricerca sul Cancro (AIRC IG 15211) to MT. Dr. Davide Branduardi (Schrodinger Inc.) is also acknowledged for insightful discussions on free-energy calculations.

ABBREVIATIONS

PPI, protein-protein interaction; EphA2, ephrin receptor A2; LCA, lithocholic acid; ELISA, enzyme-linked immunosorbent assay; META-D, metadynamics; FES, Free-energy surface; RMSD, root-mean-square deviation.

ASSOCIATED CONTENT

Experimental details and spectra (synthesis of tested compounds, ¹H and ¹³C NMR data) are reported in the Supporting Information section along with the details of the HPLC-ESI-MS/MS

analytical method. The computed coordinates of the EphA2-compound **16** complex obtained at the end of MD simulation are also available in the Supporting Information along with the analysis of the convergence of the calculated ΔA obtained by well-tempered META-D. SMILES for compounds **1-22** have been also provided in the Supporting Information.

REFERENCES

1 Himanen, J. P.; Saha, N.; Nikolov, D. B. Cell-Cell Signaling via Eph Receptors and Ephrins. *Curr. Opin. Cell. Biol.* **2007**, *19*, 534-542.

2 Pasquale, E. B. Eph-ephrin Bidirectional Signaling in Physiology and Disease. *Cell* **2008**, *133*, 38–52.

3 Pasquale, E. B. Eph Receptors and Ephrins in Cancer: Bidirectional Signalling and Beyond. *Nat. Rev. Cancer* **2010**, *10*, 165–180.

4 Wykosky, J.; Debinski, W. The EphA2 Receptor and EphrinA1 ligand in Solid Tumors: Function and Therapeutic Targeting. *Mol. Cancer Res.* **2008**, *6*, 1795–1806.

5 Boyd, A. W.; Bartlett, P. F.; Lackmann, M. Therapeutic Targeting of EPH Receptors and their Ligands. *Nat. Rev. Drug Discov.* **2014**, *13*, 39–62.

6 Ogawa, K.; Pasqualini, R.; Lindberg, R. A.; Kain, R.; Freeman, A. L.; Pasquale, E. B. The Ephrin-A1 Ligand and its Receptor, EphA2, Are Expressed During Tumor Neovascularization. *Oncogene*, **2000**; *19*, 6043–6052.

7 Margaryan, N. V.; Strizzi, L.; Abbott, D. E.; Seftor, E. A.; Rao, M. S.; Hendrix, M. J.; Hess A. R. EphA2 as a Promoter of Melanoma Tumorigenicity. *Cancer Biol. Ther.* **2009**, *8*, 279-288.

8 Tandon, M.; Vemula, S. V.; Mittal, S. K. Emerging Strategies for EphA2 Receptor Targeting for Cancer Therapeutics. *Expert Opin. Ther. Targets* **2011**, *15*, 31–51.

9 Unzue, A.; Lafleur, K.; Zhao, H.; Zhou, T.; Dong, J.; Kolb, P.; Liebl, J.; Zahler, S.; Caflisch, A.; Nevado, C. Three Stories on Eph Kinase Inhibitors: From In Silico Discovery to In Vivo Validation. *Eur. J. Med. Chem.* **2016**, *112*, 347–366.

10 Riedl, S. J.; Pasquale, E. B. Targeting the Eph System with Peptides and Peptide Conjugates. *Curr. Drug Targets* **2015**, *16*, 1031-1047.

11 Lamminmaki, U.; Nikolov, D.; Himanen, J. Eph Receptors as Drug Targets: Single-Chain Antibodies and Beyond. *Curr. Drug Targets* **2015**, *16*, 1021-1030.

12 Tognolini, M.; Hassan-Mohamed, I.; Giorgio, C.; Zanotti, I.; Lodola, A. Therapeutic Perspectives of Eph-Ephrin System Modulation. *Drug Discovery Today*. **2014**, *19*, 661-669.

13 Barquilla, A.; Pasquale, E. B. Eph Receptors and Ephrins: Therapeutic Opportunities. *Annu. Rev. Pharmacol. Toxicol.* **2015**, *55*, 465-487.

14 Castelli, R.; Tognolini, M.; Vacondio, F.; Incerti, M.; Pala, D.; Callegari, D.; Bertoni, S.; Giorgio, C.; Hassan-Mohamed, I.; Zanotti, I.; Bugatti, A.; Rusnati, M.; Festuccia, C.; Rivara, S.; Barocelli, E.; Mor, M.; Lodola, A. Δ^5 -Cholenoyl-amino Acids as Selective and Orally Available Antagonists of the Eph-ephrin System. *Eur. J. Med. Chem.* **2015**, *103*, 312-324.

15 Giorgio, C.; Hassan Mohamed, I.; Flammini, L.; Barocelli, E.; Incerti, M.; Lodola, A.; Tognolini, M. Lithocholic acid Is an Eph-Ephrin Ligand Interfering with Eph-Kinase Activation. *PloS One* **2011**, *6*, e18128.

16 Tognolini, M.; Incerti, M.; Hassan-Mohamed, I.; Giorgio, C.; Russo, S.; Bruni, R.; Lelli, B.; Bracci, L.; Noberini, R.; Pasquale, E. B.; Barocelli, E.; Vicini, P.; Mor, M.; Lodola, A. Structure-Activity Relationships and Mechanism of Action of Eph-Ephrin Antagonists: Interaction of Cholanic Acid with the EphA2 Receptor. *ChemMedChem* **2012**, *7*, 1071–1083.

17 Incerti, M.; Tognolini, M.; Russo, S.; Pala, D.; Giorgio, C.; Hassan-Mohamed, I.; Noberini, R.; Pasquale, E. B.; Vicini, P.; Piersanti, S.; Rivara, S.; Barocelli, E.; Mor, M.; Lodola, A. Amino Acid Conjugates of Lithocholic Acid as Antagonists of the EphA2 Receptor. *J. Med. Chem.* **2013**, *56*, 2936–2947.

18 Hassan-Mohamed, I.; Giorgio, C.; Incerti, M.; Russo, S.; Pala, D.; Pasquale, E. B.; Vicini, P.; Barocelli, E.; Rivara, S.; Mor, M.; Lodola, A.; Tognolini, M. UniPR129 is a Competitive Small Molecule Eph-Ephrin Antagonist Blocking In Vitro Angiogenesis at Low Micromolar Concentrations. *Br. J. Pharmacol.* **2014**, *171*, 5195-5208.

19 Hatziapostolou, M.; Polytarchou, C. Eph/ephrin System: In the Quest of Novel Anti-Angiogenic Therapies. *Br. J. Pharmacol.* **2015**, *172*, 4597–4599.

20 Tognolini, M.; Incerti, M.; Lodola, A. Are We Using the Right Pharmacological Tools to Target EphA4? *ACS Chem. Neurosci.* **2014**, *5*, 1146-1147.

21 Russo, S.; Callegari, D.; Incerti, M.; Pala, D.; Giorgio, C.; Brunetti, J.; Bracci, L.; Vicini, P.; Barocelli, E.; Capoferri, L.; Rivara, S.; Tognolini, M.; Mor, M.; Lodola, A. Exploiting Free-Energy Minima to Design Novel EphA2 Protein-Protein Antagonists: From Simulation to Experiment and Return. *Chemistry*, **2016**, *22*, 8048-8052.

22 Saleh, N.; Saladino, G.; Gervasio, F. L.; Haensele, E.; Banting, L.; Whitley, D. C., Sompova-de Oliveira Santos, J.; Bureau, R.; Clark, T. A Three-Site Mechanism for Agonist/Antagonist Selective Binding to Vasopressin Receptors. *Angew. Chem. Int. Ed. Engl.* **2016**, *55*, 8008-8012.

23 Laio, A.; Parrinello, M. Escaping Free-Energy Minima. *Proc. Natl. Acad. Sci. U. S. A.* **2002**, *99*, 12562–12566.

24 Kaus, J. W.; Harder, E.; Lin, T.; Abel, R.; Mc Cammon, J. A.; Wang, L. How to Deal with Multiple Binding Poses in Alchemical Relative Protein-Ligand Binding Free Energy Calculations. *J. Chem. Theory Comput.* **2015**, *11*, 2670-2679.

25 Gkeka, P.; Eleftheratos, S.; Kolocouris, A.; Cournia, Z. Free Energy Calculations Reveal the Origin of Binding Preference for Aminoadamantane Blockers of Influenza A/M2TM Pore. *J. Chem. Theory Comput.* **2013**, *9*, 1272-1281.

26 Kuhnert, M.; Köster, H.; Bartholomäus, R.; Park, A. Y.; Shahim, A.; Heine, A.; Steuber, H.; Klebe, G.; Diederich, W. E. Tracing Binding Modes in Hit-to-Lead Optimization: Chameleon-like Poses of Aspartic Protease Inhibitors. *Angew. Chem. Int. Ed. Engl.* **2015**, *54*, 2849-2853.

27 Prathipati, P.; Nagao, C.; Ahmad, S.; Mizuguchi, K. Improved Pose and Affinity Predictions Using Different Protocols Tailored on the Basis of Data Availability. *J. Comput. Aided Mol. Des.* **2016**, *30*, 817-828.

28 Janssen, F. J.; Baggelaar, M. P.; Hummel, J. J.; Overkleeft, H. S.; Cravatt, B. F.; Boger, D. L.; van der Stelt, M. Comprehensive Analysis of Structure-Activity Relationships of α -

Ketoheterocycles as sn-1-Diacylglycerol Lipase α Inhibitors. *J. Med. Chem.* **2015**, *58*, 9742-9753.

29 Clark, A. J.; Tiwary, P.; Borrelli, K.; Feng, S.; Miller, E. B.; Abel, R.; Friesner, R. A.; Berne, B. J. Prediction of Protein-Ligand Binding Poses via a Combination of Induced Fit Docking and Metadynamics Simulations. *J. Chem. Theory Comput.* **2016**, *12*, 2990-2998.

30 De Vivo, M.; Masetti, M.; Bottegoni, G.; Cavalli, A. Role of Molecular Dynamics and Related Methods in Drug Discovery. *J. Med. Chem.* **2016**, *59*, 4035-4061.

31 Gervasio, F. L.; Laio, A.; Parrinello, M. Flexible Docking in Solution Using Metadynamics. *J. Am. Chem. Soc.* **2005**, *127*, 2600-2607.

32 Masetti, M.; Cavalli, A.; Recanatini, M.; Gervasio, F. L. Exploring Complex Protein-Ligand Recognition Mechanisms with Coarse Metadynamics. *J. Phys. Chem. B* **2009**, *113*, 4807-4816.

33 Grazioso, G.; Limongelli, V.; Branduardi, D.; Novellino, E.; De Micheli, C.; Cavalli, A.; Parrinello, M. Investigating the Mechanism of Substrate Uptake and Release in the Glutamate Transporter Homologue Glt_{Ph} through Metadynamics Simulations. *J. Am. Chem. Soc.* **2012**, *134*, 453-463.

34 Sinko, W.; Lindert, S.; McCammon, J. A. Accounting for Receptor Flexibility and Enhanced Sampling Methods in Computer-Aided Drug Design. *Chem. Biol. Drug Des.* **2013**, *81*, 41-49.

35 Palermo, G.; Minniti, E.; Greco, M. L.; Riccardi, L.; Simoni, E.; Convertino, M.; Marchetti, C.; Rosini, M.; Sissi, C.; Minarini, A.; De Vivo, M. An Optimized Polyamine Moiety Boosts the Potency of Human Type II Topoisomerase Poisons as Quantified by Comparative Analysis Centered on the Clinical Candidate F14512. *Chem. Commun.* **2015**, *51*, 14310–14313.

36 Duffy, E. M.; Jorgensen, W. L. Prediction of Properties from Simulations: Free Energies of Solvation in Hexadecane, Octanol, and Water. *J. Am. Chem. Soc.* **2000**, *122*, 2878- 2888.

37 Bissantz, C.; Kuhn, B.; Stahl, M. A Medicinal Chemist's Guide to Molecular Interactions. *J. Med. Chem.* **2010**, *53*, 5061-5084.

38 *QikProp*, Schrödinger, LLC, New York, NY, 2016.

39 Himanen, J. P.; Goldgur, Y.; Miao, H.; Myshkin, E.; Guo, H.; Buck, M.; Nguyen, M.; Rajashankar, K. R.; Wang, B.; Nikolov, D. B. Ligand Recognition by A-Class Eph Receptors: Crystal Structures of the EphA2 Ligand-Binding Domain and the EphA2/ephrin-A1 complex. *EMBO Rep.* **2009**, *10*, 722-728.

40 Zhao, H.; Caflisch, A. Molecular Dynamics in Drug Design. *Eur. J. Med. Chem.* **2015**, *91*, 4-14.

41 Spyrakis, F.; Bidon Chanal, A.; Barril, X.; Luque, F. J. Protein Flexibility and Ligand Recognition: Challenges for Molecular Modeling. *Curr. Top. Med. Chem.* **2011**, *11*, 192–210.

42 Friesner, R. A.; Banks, J. L.; Murphy, R. B.; Halgren, T. A.; Klicic, J. J.; Mainz, D. T.; Repasky, M. P.; Knoll, E. H.; Shaw, D. E.; Shelley, M.; Perry, J. K.; Francis, P.; Shenkin, P. S.

Glide: A New Approach for Rapid, Accurate Docking and Scoring. 1. Method and Assessment of Docking Accuracy, *J. Med. Chem.* **2004**, *47*, 1739–1749.

43 Barducci, A.; Bussi, G.; Parrinello, M. Well-tempered Metadynamics: A Smoothly Converging and Tunable Free-Energy Method. *Phys. Rev. Lett.* **2008**, *100*, 020603.

44 Limongelli, V.; Marinelli, L.; Cosconati, S.; La Motta, C.; Sartini, S.; Mugnaini, L.; Da Settimo, F.; Novellino, E.; Parrinello, M. Sampling Protein Motion and Solvent Effect During Ligand Binding. *Proc. Natl. Acad. Sci. U. S. A.* **2012**, *109*, 1467-1472.

45 Limongelli, V.; Bonomi, M.; Marinelli, L.; Gervasio, F. L.; Cavalli, A.; Novellino, E.; Parrinello, M. Molecular Basis of Cyclooxygenase Enzymes (COXs) Selective Inhibition. *Proc. Natl. Acad. Sci. U. S. A.* **2010**, *107*, 5411–5416.

46 Saladino, G.; Gauthier, L.; Bianciotto, M.; Gervasio, F. L. Assessing the Performance of Metadynamics and Path Variables in Predicting the Binding Free Energies of p38 Inhibitors. *J. Chem. Theory Comput.* **2012**, *8*, 1165–1170.

47 Valsami, G.; Macheras, P. Computational-Regulatory Developments in the Prediction of Oral Drug Absorption. *Mol. Inform.* **2011**, *2*, 112-121.

48 Lipinski, C.A. Rule of five in 2015 and beyond: Target and Ligand Structural Limitations, Ligand Chemistry Structure and Drug Discovery Project Decisions. *Adv. Drug Deliv. Rev.* **2016** *101*, 34-41.

49 *Maestro*, version 10.5; Schrödinger, LLC, New York, NY, 2016.

50 *Glide*, version 7.0, Schrödinger, LLC, New York, NY, 2016.

51 Banks, J.L.; Beard, H.S.; Cao, Y.; Cho, A.E.; Damm, W.; Farid, R.; Felts, A.K.; Halgren, T.A.; Mainz, D.T.; Maple, J.R.; Murphy, R.; Philipp, D.M.; Repasky, M.P.; Zhang, L.Y.; Berne, B.J.; Friesner, R.A.; Gallicchio, E.; Levy, R.M. Integrated Modeling Program, Applied Chemical Theory (IMPACT). *J. Comp. Chem.* **2005**, *26*, 1752-1780.

52 Darden, T.; York, D.; Pedersen, L. Particle Mesh Ewald: An N Log (N) Method for Ewald Sums in Large Systems. *J. Chem. Phys.* **1993**, *98*, 10089–10092.

53 Loncharich, R. J.; Brooks, B. R.; Pastor, R. W. Langevin Dynamics of Peptides: The Frictional Dependence of Isomerization Rates of N-acetylalanyl-N'-methylamide. *Biopolymers* **1992**, *32*, 523-535.

54 (a) *Desmond Molecular Dynamics System*, version 4.5; D. E. Shaw Research: New York, 2016; (b) *Maestro–Desmond Interoperability Tools*, version 4.5; Schrödinger: New York, 2016.

55 Fidelak, J.; Juraszek, J.; Branduardi, D.; Bianciotto, M.; Gervasio, F. L. Free-Energy-Based Methods for Binding Profile Determination in a Congeneric Series of CDK2 Inhibitors. *J. Phys. Chem. B* **2010**, *114*, 9516–9524.

Table of Contents graphic (TOC)

